Granular Matter (2012) 14:51–61
DOI 10.1007/s10035-011-0298-8

ORIGINAL PAPER

Granular element method (GEM): linking inter-particle forces with macroscopic loading

José E. Andrade · Carlos F. Avila

Received: 23 March 2011 / Published online: 2 December 2011

Abstract We present a new method capable of inferring, for the first time, inter-particle contact forces in irregularly-shaped natural granular materials (e.g., sands), using basic Newtonian mechanics and balance of linear momentum at the particle level. The method furnishes a relationship between inter-particle forces and corresponding average particle stresses, which can be inferred, for instance, from measurements of average particle strains emanating from advanced experimental techniques (e.g., 3D X-ray diffraction). Inter-particle forces are the missing link in understanding how forces are transmitted in complex granular structures and the key to developing physics-based constitutive models. We present two numerical examples to verify the method and showcase its promise.

Keywords Granular element method · Contact forces · Discrete mechanics · Multiscale modeling

1 Introduction

Granular materials are misleadingly simple: their fundamental behavior is represented by individual grains that, collectively, dictate the macroscopic behavior of the material. Engineering practice has struggled to model the collective or macroscopic behavior of granular materials using continuum mechanics and phenomenomenological elastoplasticity has become the framework of choice (e.g., [1–8]). Elastoplasticity has been very successful in engineering practice and will likely continue to occupy an important role in the forseeable future. However, it seems like phenomenology has reached a glass ceiling and progress is becoming incremental. On the other hand, a discrete approach was proposed by Cundall and Strack [9] and it was predicated on the purity of modeling material behavior starting from the basic granular scale. Discrete models rely on more basic physics (e.g., Newtonian mechanics for large particles) [10–13] but have been unable to represent complex particle geometries and, as a result, have not yet been able to provide engineering science with quantitative predictions.

From the experimental perspective, new technologies are enabling unprecedented access to information at lower scales that have not been considered possible a few years ago. Progress has been made in unraveling much of the kinematic processes in granular matter (mostly owing to X-ray CT) [14–17], but progress in the area of natural inter-granular contact forces remains sparse [18]. For example, it is now possible to obtain full field kinematics in sand particles as they are loaded macroscopically [19]. Using X-ray CT, it is hence possible to obtain all six degrees of freedom in each particle, for thousands of particles constituting a macroscopic assembly. Multiscale models capable of using these incredibly rich kinematics have very recently emerged [20].

In the area of inter-particle forces, new developments using 3D X-ray diffraction (3DXRD) [21] have shown that it is possible to measure average elastic strains in sand particles under macroscopic loading [22]. A fundamental question immediately emerges: is there a link between measurable average strains in granular materials and inter-granular contact forces? If the constitutive response (e.g., elasticity) of the particle is known, one can calculate average stress on each particle. Could these stresses link to inter-granular contact forces? This paper aims at answering this question.

The ability to measure inter-particle forces in natural granular materials is the missing link to constructing physics-based constitutive models and multiscale models.

J. E. Andrade (✉) · C. F. Avila
Division of Engineering and Applied Science, California Institute of Technology, Pasadena, CA 91125, USA
e-mail: jandrade@caltech.edu

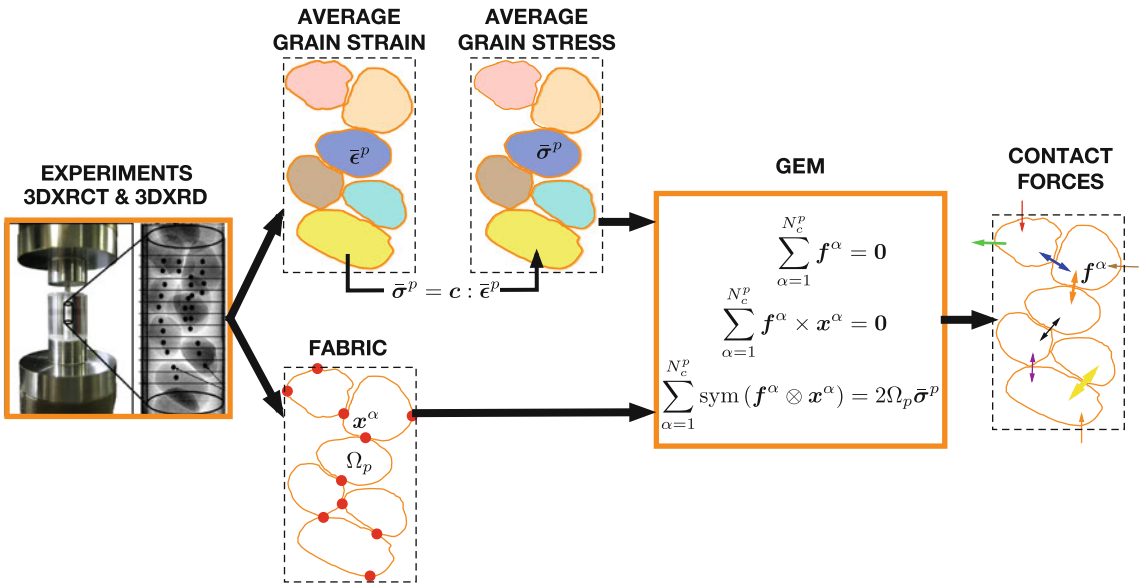

Fig. 1 GEM concept. Average particle strains can be measured using 3DXRD and fabric information (particle shape and contact point location) can be extracted using 3DXRCT while granular materials are being loaded macroscopically. Using particles as strain gauges, one can use a constitutive relation (linear or non-linear) to compute average particle stresses from average particle strains. Average particle stresses and fabric (plus boundary conditions) are taken as input by GEM to infer inter-particle contact forces in general granular materials under macroscopic loading. Picture on the left taken from [22]

The relationship between inter-granular forces and macroscopic stresses has been known for decades [23]. However, our ability to measure inter-granular forces in general natural granular materials has been missing. Photoelasticity was a tremendous contribution to this question, but is limited to birefringent materials [24,25] and hence cannot be applied to natural granular materials such as sands. Furthermore, as explained in [26,27], photoelasticity produces contours measuring the difference between principal stresses. Therefore, an infinite set of forces can be found to satisfy photoelastic measurements. The combination of 3DXRD with a method that can produce inter-particle contact forces from average particle stresses could fill the current gap.

In this paper, we propose a new computational technique called the granular element method (GEM) that takes information about the fabric of the granular material and the average stresses in particles as input, and produces the inter-particle contact forces as output. We also connect these inter-particle forces with macroscopic average stresses in assemblies of particles, hence furnishing a multiscale bridge. The method is based on Newtonian mechanics and balance of linear momentum at the particle level. These set of equations produce a system that can solve for the contact forces in an otherwise statically indeterminate problem. In essence, the method relies on established mechanical principles: it combines Newtonian mechanics with balance of linear momentum at the particle level. Furthermore, when combined with experimental measurements of average strains (e.g., from 3DXRD), the method would rely on Hooke's law to transform average strains into average stresses. Similar concepts have been independently used in structural mechanics [28]. It is the novel exploitation of the consequences emanating from these established mechanics principles that make GEM original. The essence of the proposed GEM technique is showcased in Fig. 1, with its main ingredients further explicated in the subsequent sections of this paper. It is shown here that this simple method can reconstruct the force network in granular assemblies under quasi-static loading, for general grain shapes, and various degrees of inter-particle friction. GEM could be used in conjunction with 3DXRD by essentially using particles as strain gauges by measuring average strains that can be then converted to average stresses. This concept is highlighted in the numerical examples.

The structure of the paper is as follows. First, we recall basic Newtonian mechanics at the particle level by enforcing static equilibrium and balance of linear momentum inside each particle. We relate the balance of linear momentum to the average stress and use continuum mechanics to connect the average stress with contact forces on particle boundaries. Then we present the granular element method (GEM) as a computational framework exploiting Newtonian mechanics to obtain the inter-particle forces in a particle array, provided the fabric and average granular stresses are known. We also connect the resulting inter-particle forces with average macroscopic stresses in the particle assembly. Finally, we present some examples that showcase the promise and capability of the method. In particular, we present an example where particle fabric and average particle strains are obtained from a

finite element simulation, in a fundamentally similar way to the process to be followed experimentally using 3DXRCT and 3DXRD, and then passed to GEM to infer inter-particle contact forces. This example showcases the applicability of the new GEM method, in combination with advanced experimental techniques where particle fabric and average particle strains can be measured as a function of macroscopic loading, in order to infer, for the first time, inter-particle contact forces in opaque natural granular materials such as sands. In essence, this example replaces the far-left side of Fig. 1 with calculations using finite elements to showcase the usability of the GEM procedure.

As for notations and symbols used in this paper, bold-faced letters denote tensors and vectors; the symbol '$\cdot$' denotes an inner product of two vectors (e.g. $\boldsymbol{a}\cdot\boldsymbol{b} = a_i b_i$), or a single contraction of adjacent indices of two tensors (e.g. $\boldsymbol{c}\cdot\boldsymbol{d} = c_{ij}d_{jk}$); the symbol ':' denotes an inner product of two second-order tensors (e.g. $\boldsymbol{c} : \boldsymbol{d} = c_{ij}d_{ij}$), or a double contraction of adjacent indices of tensors of rank two and higher (e.g. $\boldsymbol{C} : \boldsymbol{\epsilon}^{\mathrm{e}} = C_{ijkl}\epsilon^{\mathrm{e}}_{kl}$); the symbol '$\otimes$' denotes a juxtaposition, e.g., $(\boldsymbol{a}\otimes\boldsymbol{b})_{ij} = a_i b_j$. For any symmetric second order tensors $\boldsymbol{\alpha}$ and $\boldsymbol{\beta}$, $(\boldsymbol{\alpha}\otimes\boldsymbol{\beta})_{ijkl} = \alpha_{ij}\beta_{kl}$, $(\boldsymbol{\alpha}\oplus\boldsymbol{\beta})_{ijkl} = \alpha_{ik}\beta_{jl}$, and $(\boldsymbol{\alpha}\ominus\boldsymbol{\beta})_{ijkl} = \alpha_{il}\beta_{jk}$. Finally, the symmetry operator extracts the symmetric part of a second order tensor $\boldsymbol{\epsilon}$ such that $\mathrm{sym}\,\boldsymbol{\epsilon} = 1/2\left(\epsilon_{ij} + \epsilon_{ji}\right)$.

2 Granular Newtonian mechanics

Our point of departure for the granular element method (GEM) is quasi-static conditions. It should be noted though that the method can be extended to fully dynamic loadings. Taking a particle point of view, Euler's equations for the case of static equilibrium of a particle Ω_p read

$$\sum_{\alpha=1}^{N_c^p} \boldsymbol{f}^{\alpha} = \boldsymbol{0} \tag{1}$$

$$\sum_{\alpha=1}^{N_c^p} \boldsymbol{f}^{\alpha} \times \boldsymbol{x}^{\alpha} = \boldsymbol{0} \tag{2}$$

where the first equation requires all N_c^p contact forces exerted on particle Ω_p to collectively vanish and the second equation requires the sum of moments to vanish. The vector $\boldsymbol{x}^{\alpha}$ defines the distance from the origin to the point of application of contact force $\boldsymbol{f}^{\alpha}$. Figure 2 shows a pictorial description of the point forces and distance vectors for a typical particle Ω_p. We should note that we have assumed here that contact is transmitted at points. This is a relatively good assumption for stiff materials (e.g., silica) at relatively low pressures.

In addition to Euler's equations of static equilibrium, one can require that balance of linear momentum is satisfied for a given particle Ω_p, where Ω_p is the set of points defining

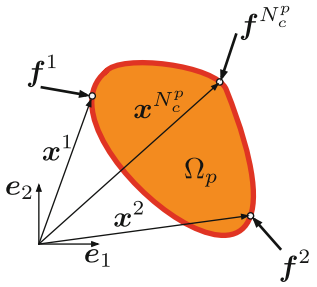

Fig. 2 Single-grain schematic depicting contact (*point*) forces and contact point positions relative to an inertial reference frame

the domain of particle p, which is defined as an area or a volume, if in 2D or 3D, respectively. Linear momentum within particle Ω_p under quasi-static conditions requires

$$\nabla^{\boldsymbol{x}}\cdot\boldsymbol{\sigma} = \boldsymbol{0} \qquad \forall \boldsymbol{x} \in \Omega_p \tag{3}$$

where $\boldsymbol{\sigma}$ is the point-wise stress tensor and where we have neglected body forces. In this context, point-wise signifies a tensor field that is defined at every point $\boldsymbol{x}$ on the domain Ω_p. Furthermore, we will henceforth assume small deformations within the particles. Clearly, this does not preclude grains from sliding significantly. By the same token, one can define the average stress $\bar{\boldsymbol{\sigma}}^p$ within particle Ω_p such that

$$\bar{\boldsymbol{\sigma}}^p := \frac{1}{\Omega_p}\int_{\Omega_p} \boldsymbol{\sigma}\,\mathrm{d}\Omega_p \tag{4}$$

Using Eq. (3), we can obtain the identity $\boldsymbol{\sigma} = \nabla^{\boldsymbol{x}}\cdot(\boldsymbol{\sigma}\otimes\boldsymbol{x})$ for $\boldsymbol{x} \in \Omega_p$. Using the definition of traction related to point forces, we obtain $\boldsymbol{t}^{\alpha}\mathrm{d}\Gamma_p = \mathrm{d}\boldsymbol{f}^{\alpha}$, where $\mathrm{d}\Gamma_p$ is an infinitesimal surface element of the particle. Finally, invoking Cauchy's stress theorem [29], relating tractions and stresses on a plane, i.e., $\boldsymbol{t} = \boldsymbol{\sigma}\cdot\boldsymbol{n}$, where $\boldsymbol{n}$ is the unit vector normal to the plane, we get a direct relationship between the average stress at a particle and the point-forces via the divergence theorem, i.e.,

$$\bar{\boldsymbol{\sigma}}^p = \frac{1}{\Omega_p}\sum_{\alpha=1}^{N_c^p} \mathrm{sym}\left(\boldsymbol{f}^{\alpha}\otimes\boldsymbol{x}^{\alpha}\right) \tag{5}$$

where we note the use of the symmetry operator 'sym', which results from the symmetry of the point-wise stress tensor $\boldsymbol{\sigma}$.

Remark 1 Note that Eq. (3) is appropriately defined as the equilibrium equation *within* a particle (volume or area) Ω_p. At the grain-scale, continuum mechanics applies and Eqs. (3)–(5) hold. At the meso-scale (looking at groups of particles) discontinuities arise and the application of continuum mechanics requires the notion of averaging over representative volumes, see Sect. 4.

Consequently, Eqs. (1), (2), and (5) constitute a set of linear equations for each particle Ω_p. We should remark that

these relations are linear equations of the point forces exerted on the boundary Γ_p of particle Ω_p and, consequently, if the location $\boldsymbol{x}^\alpha$ of the contact points is known and the average stress $\bar{\boldsymbol{\sigma}}^p$ in the particle is known, then we can use this set of equations to directly solve for the contact forces $\boldsymbol{f}^\alpha$. If the number of spatial dimensions is N_{sd}, we get $N_{sd}(N_{sd}+1)$ linear scalar equations in each particle. Therefore, if a particle point of view is taken, one can solve for at most $N_{sd}+1$ contact forces on the boundary of a particle Ω_p. However, using Newton's third law, we will be able to solve for more forces once we account for the entire particle array.

Remark 2 Recent publications using advanced experimental techniques combining 3D X-ray CT and 3D X-ray diffraction [22] show the real possibility of measuring the fabric of granular materials (here fabric is defined as the shape of grains and contact point locations) as well as the average elastic strains within particles. When these advances reach their full potential, analysts and experimentalists will be able to use GEM to infer the value of inter-particle contact forces in granular assemblies under macroscopic loading. This concept is illustrated in Fig. 1. The basic notion is to use particles as local strain gauges, essentially using the concept of force. Every experimentalist knows that forces cannot be measured, rather, they are inferred from deformations emanating from 'known' elastic processes. In the case of GEM, if the constitutive behavior of the particles is known, one can calculate average stresses using generalized Hooke's law such that $\bar{\boldsymbol{\sigma}}^p = \boldsymbol{c} : \bar{\boldsymbol{\epsilon}}^p$, where $\bar{\boldsymbol{\epsilon}}^p$ is the average elastic strain tensor at a particle (e.g., as measured using 3DXRD in [22]) and $\boldsymbol{c}$ is the elastic stiffness of the particle, which is assumed known for most practical purposes where elasticity applies (e.g., no particle breakage, etc.). It should be noted that linear elasticity is not required by GEM. Any stress-strain (linear or non-linear) relation of the form given above can be used. At that point, we will be able to obtain full grain-scale kinematics *and* grain-scale particle contact forces for real granular assemblies under macroscopic loading. This constitutes the missing link in multiscale analysis for granular materials connecting the macro scale with the fundamental grain scale. GEM furnishes a crucial bridge to establish this fundamental and promising connection in the near future.

Remark 3 The central ingredient of the proposed GEM framework is to link average particle stresses and inter-particle forces as expressed in Eq. (5). This linkage essentially overcomes the issue of static indeterminacy in granular assemblies. It should be noted that this could also be achieved by other experimental methods such as that presented in [25] where the inter-particle forces are estimated by matching maximum shear stress contours obtained from two-dimensional photoelasticity. Nevertheless, photoelasticity only works in birefringent materials and the forces obtained are not unique [26,27].

3 Granular element method (GEM)

The granular element method (GEM) uses the fundamental mechanics equations derived in the previous section, in particular Eqs. (1), (2), and (5), to solve for the contact forces in a granular assembly of particles. The method assumes that the location of the contact points is known (e.g., as measured from 3DXRCT) and that the average stress (or strain) in each particle is given (e.g., as measured from 3DXRD). Without loss of generality, and for clarity of presentation, we adopt a two-dimensional approach henceforth. The fundamental mechanics equations at a particle Ω_p can be written in matrix form such that

$$\sum_{\alpha=1}^{N_c^p} \boldsymbol{K}^\alpha \cdot \boldsymbol{f}^\alpha = \boldsymbol{b}^p \tag{6}$$

where, in 2D, the matrices take the explicit form

$$\boldsymbol{K}^\alpha = \begin{bmatrix} 1 & 0 \\ 0 & 1 \\ x_2^\alpha & -x_1^\alpha \\ x_1^\alpha & 0 \\ 0 & x_2^\alpha \\ x_2^\alpha & x_1^\alpha \end{bmatrix}; \quad \boldsymbol{f}^\alpha = \begin{Bmatrix} f_1^\alpha \\ f_2^\alpha \end{Bmatrix}; \quad \boldsymbol{b}^p = \begin{Bmatrix} 0 \\ 0 \\ 0 \\ \Omega_p \bar{\sigma}_{11}^p \\ \Omega_p \bar{\sigma}_{22}^p \\ 2\Omega_p \bar{\sigma}_{12}^p \end{Bmatrix} \tag{7}$$

where we have expressed the positions for the contact forces and the average particle stresses in components. It should be emphasized that $\boldsymbol{K}^\alpha$ and $\boldsymbol{b}^p$ are known since GEM assumes that the location of contacts and the average particle stresses are known. By simple expansion Eq. (6) can be shown to encapsulate Eqs. (1), (2), and (5). For instance, the top two rows of the two dimensional case presented above, correspond to balance of forces, while the third row enforces balance of moments, and the last three enforce the equations of average stress at the particle level.

Remark 4 As mentioned above, the granular element method assumes the location of contact points and the average particle stresses as known information. In the current context, this information is envisioned as being provided by experimental measurements such as 3DXRCT and 3DXRD, however, one can imagine combining GEM with other computational or analytical methods such as finite elements or discrete elements such as that presented in [30]. In fact, in the examples presented herein, the method is combined with finite element and discrete element calculations to show its applicability.

Remark 5 It should be emphasized that, as shown in Fig. 1, the granular element method presented herein is not a standalone computational method. On the contrary, it is designed to work in conjunction with an experimental or computational method where the average stresses (or strains) are measured and passed to GEM. This should be contrasted with

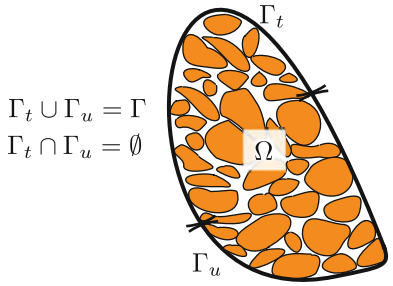

Fig. 3 Assembly of particles Ω with a boundary defined by Γ. Boundary can be loaded macroscopically and is split into a region where stresses or tractions are prescribed Γ_t and a region where tractions are unknown Γ_u (reactions)

other computational methods such as DEM, contact dynamics, or finite elements, where the inter-particle contact forces are directly computed, independently. The attractiveness of GEM is to provide a method to eventually infer inter-particle contact forces directly from experimental measurements, as shown in Fig. 1 and as showcased in the numerical experiments presented in this paper. The use of the particles themselves as strain gauges is a key feature of GEM.

Now, consider an array of N_p particles under general macroscopic loading as shown in Fig. 3. In addition, let the N_p-particle array have N_c total number of contact points. As observed in Fig. 3, the array is defined by a boundary Γ, which defines the bounds of the macroscopic domain Ω. As in classic solid deformation analysis, the boundary of the domain is decomposed into a portion Γ_t where forces (tractions) are prescribed, and a complement Γ_u where forces are not prescribed and need to be determined. These forces are treated in GEM as contact forces, but they are not inter-particle contact forces as they reside on the boundary Γ. Borrowing from finite element technology [31], let the set $\eta = \{1, 2, \ldots, N_c\}$ denote the set of global contact point numbers. Let $\eta_{gi} \subset \eta$ be the set of nodes at which the i-th component of force is prescribed, and let $\eta - \eta_{gi}$ be the complement of η_{gi}. Henceforth we refer to set $\eta_A := \eta - \eta_{gi}$ as the active set and η_{gi} as the prescribed or inactive set for $i = 1, \ldots, N_{sd}$.

The method also exploits action and reaction for inter-particle contacts. Therefore, each inter-particle contact is shared between two particles, one is called the master and the other the slave. If the α-th contact is shared between particles Ω_p and Ω_q, then the force exerted on particle Ω_p is $\boldsymbol{f}^\alpha$ and that exerted on particle Ω_q is $-\boldsymbol{f}^\alpha$. This enables us to define the global vector of active contact forces in the assembly as $\boldsymbol{f}$. Clearly, each spatial dimension can have a different set of active contact points. In other words $\eta - \eta_{gi}$ are, in general, different sets for $i = 1, \ldots, N_{sd}$, just as in general solid mechanics. It should be emphasized that $\boldsymbol{f}$ contains all the active forces in the particle array. Therefore, the mechanics equations for each particle defined in Eq. (6) can be written in terms of the global active forces such that

$$\boldsymbol{K}^p \cdot \boldsymbol{f} = \hat{\boldsymbol{b}}^p \tag{8}$$

where $\boldsymbol{K}^p$ is called the particle matrix and is assembled using all active forces on particle Ω_p and $\hat{\boldsymbol{b}}^p = \boldsymbol{b}^p - \sum_{\beta \in \eta_{gi}} \boldsymbol{K}^\beta(:, i) f_i^\beta$ is the modified particle forcing vector, where the contribution of the prescribed set is taken into account. Letting the number of unknown or active forces be N_u, then the dimensions of the active force vector $\boldsymbol{f}$ are $N_u \times 1$ and the dimensions for the particle matrix $\boldsymbol{K}^p$ are $N_{sd}(N_{sd}+1) \times N_u$. Equation (8) yields $N_{sd}(N_{sd}+1)$ linear equations per particle as before, but unlike (6), it is written in terms of the global active force vector $\boldsymbol{f}$.

Finally, we can consider each of the N_p particles in the array and obtain a system of $N_p(N_{sd})(N_{sd}+1)$ equations for the whole array, i.e.,

$$\boldsymbol{K} \cdot \boldsymbol{f} = \boldsymbol{b} \tag{9}$$

where

$$\boldsymbol{K} = \begin{bmatrix} \boldsymbol{K}^1 \\ \boldsymbol{K}^2 \\ \vdots \\ \boldsymbol{K}^{N_p} \end{bmatrix}; \quad \boldsymbol{b} = \begin{Bmatrix} \hat{\boldsymbol{b}}^1 \\ \hat{\boldsymbol{b}}^2 \\ \vdots \\ \hat{\boldsymbol{b}}^{N_p} \end{Bmatrix} \tag{10}$$

The equations encapsulated in (9) result in a rectangular system of $N_p(N_{sd})(N_{sd}+1)$ equations with N_u unknowns. The number of unknowns depends on the boundary conditions imposed, but in general, $N_u \leq N_{sd}(N_c)$. For rectangular systems, there are many possibilities [32]: there may be infinitely many solutions for every $\boldsymbol{b}$; or infinitely many for some $\boldsymbol{b}$ and no solution for others; or one solution for some $\boldsymbol{b}$ and none for others. If we require more equations than unknowns, this is satisfied if $N_c/N_p \leq N_{sd}+1$. When this is the case, and if the columns are linearly independent, the force vector $\boldsymbol{f}$ will have no free variables and if there exists a solution, this solution will be unique. However, there will be cases where this solution does not exist since $\boldsymbol{b}$ may not be in the column space of $\boldsymbol{K}$. This can occur, for example, if there are errors in measuring average stresses in particles, or prescribed boundary forces, which all contribute to the right-hand side of the system. In general granular assemblies, $\boldsymbol{K}$ has N_u linearly independent columns.

Figure 4 shows a simple example of the topology of the different arrays involved in the granular element method. The top part of the figure shows a typical configuration where two particles Ω_p and Ω_q are in contact at point α. Additionally, particle Ω_p is in contact with the boundary of the array and is subjected to a prescribed force $\boldsymbol{f}^\beta$ and a reaction force $\boldsymbol{f}^\gamma$. The active force array $\boldsymbol{f}$ is depicted at the bottom of the figure and shows the contribution of the unknown forces $\boldsymbol{f}^\alpha$ (inter-particle contact) and $\boldsymbol{f}^\gamma$ (contact force at the boundary). One can also observe that contact α has a master particle Ω_p and a slave particle Ω_q. Contact point (and force) α is an

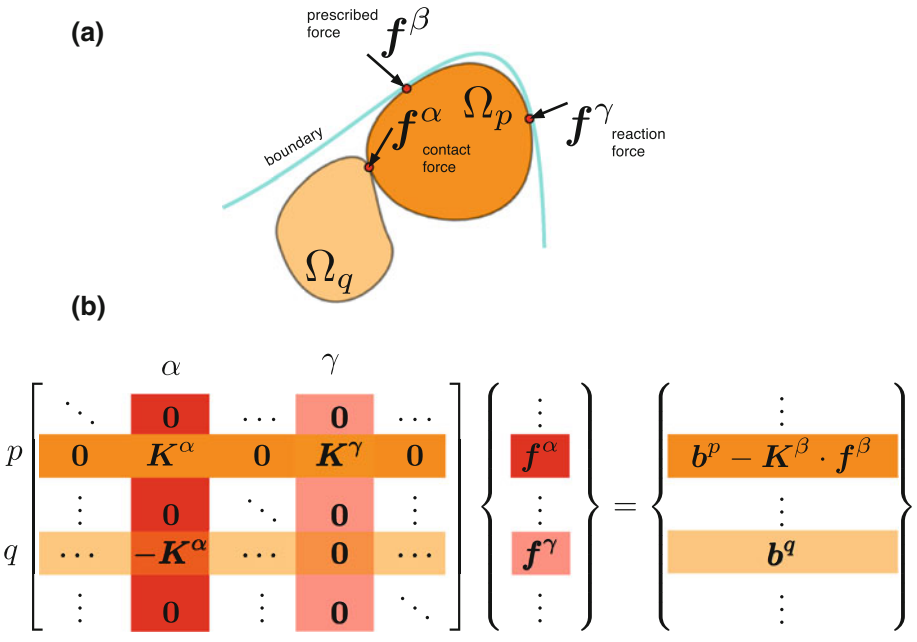

Fig. 4 Example of **a** typical forces encountered in GEM and **b** their contributions to the topology of the global stiffness $\boldsymbol{K}$ and forcing vector $\boldsymbol{b}$

inter-particle contact and it is shared by two particles, hence the contribution with $\boldsymbol{K}^\alpha$ to the p-th particle (row) and α-th contact (column) of the global stiffness matrix $\boldsymbol{K}$, and $-\boldsymbol{K}^\alpha$ for the q-th row and α-th column. All other entries in the α-th column are zero. Similarly, $\boldsymbol{K}^\gamma$ is the only non-zero contribution to the γ-th column of the matrix $\boldsymbol{K}$, corresponding to the p-th particle row. Finally, boundary particles with prescribed forces must account for this effect on the right-hand side as depicted for $\boldsymbol{f}^\beta$.

Remark 6 Similar to the finite element method (FEM) [31, 33], each particle can be seen as an 'element' with contact points serving as 'nodes'. These 'nodes' are shared with adjacent grains if they are inter-particle contacts. Nodes contribute to the element stiffnesses if they are active and belong to that particle. Also, element (grain) stiffnesses contribute to the global stiffness of the system $\boldsymbol{K}$. Prescribed forces at nodes contribute to the right-hand side of the system. However, unlike FEM, GEM does not yield square matrices and may not have a solution (e.g., due to experimental measurement errors). When this is the case, the method will only provide approximate solutions, using singular value decomposition (SVD), for example.

4 Multiscale considerations

The measurement or inference of inter-particle contact forces opens the door to the development of more physics-based constitutive models for engineering purposes. To this end, GEM can provide the missing link to calculate macroscopic average stresses for a granular assembly based on the micromechanical inter-particle forces and the fabric of the array.

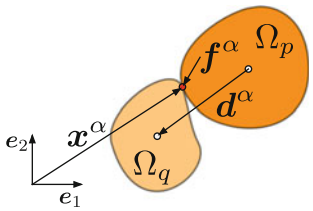

Fig. 5 Two prototypical particles in contact at point $\boldsymbol{x}^\alpha$. Each particle has a centroid and they are connected by the branch vector $\boldsymbol{d}^\alpha$

The theoretical foundations are not new and we consolidate previous developments with those presented herein for clarity and for completion.

Let us define the average macroscopic stresses in a volumetric assembly of granular materials so that (cf., Fig. 3)

$$\langle \boldsymbol{\sigma} \rangle := \frac{1}{\Omega} \int_\Omega \boldsymbol{\sigma} \, \mathrm{d}\Omega \equiv \frac{1}{\Omega} \sum_{p=1}^{N_p} \Omega_p \bar{\boldsymbol{\sigma}}^p \tag{11}$$

where we have used the fact that, under drained conditions, the stress $\boldsymbol{\sigma}$ is only non-zero inside particles. Using this definition, and replacing the definition of average particle stresses in Eq. (5) we get

$$\langle \boldsymbol{\sigma} \rangle = \frac{1}{\Omega} \sum_{p=1}^{N_p} \sum_{\alpha=1}^{N_c^p} \mathrm{sym} \left(\boldsymbol{f}^\alpha \otimes \boldsymbol{x}^\alpha \right) \tag{12}$$

This last expression can be written in more compact form by exploiting action and reaction, and by defining the so-called branch vectors. Figure 5 shows two particles in contact at $\boldsymbol{x}^\alpha$. The branch vectors join the centroids of the particles and can be defined as $\boldsymbol{d}^\alpha = \boldsymbol{x}^q - \boldsymbol{x}^p$, where $\boldsymbol{x}^q$ and $\boldsymbol{x}^p$ represent the

position for the centroid of the Ω_q and Ω_p particle, respectively. Additionally, the contact point $\boldsymbol{x}^\alpha = \boldsymbol{x}^p + \boldsymbol{x}^{\alpha,p} = \boldsymbol{x}^q + \boldsymbol{x}^{\alpha,q}$, where $\boldsymbol{x}^{\alpha,p}$ and $\boldsymbol{x}^{\alpha,q}$ represent the vector from the centroid of particle Ω_p to the contact point $\boldsymbol{x}^\alpha$ and that from Ω_q to $\boldsymbol{x}^\alpha$, respectively. Using this vectorial identities, and Eqs. (1) and (12), we obtain the identity

$$\langle \boldsymbol{\sigma} \rangle = \frac{1}{\Omega} \sum_{p=1}^{N_p} \sum_{\alpha=1}^{N_c^p} \operatorname{sym} \left(\boldsymbol{f}^\alpha \otimes \boldsymbol{x}^\alpha \right) \equiv \frac{1}{\Omega} \sum_{\alpha=1}^{N_c} \operatorname{sym} \left(\boldsymbol{f}^\alpha \otimes \boldsymbol{d}^\alpha \right) \tag{13}$$

where the latter expression was proposed by Christoffersen et al. [23] and provides a compact relationship between the macroscopic average stress $\langle \boldsymbol{\sigma} \rangle$ and the inter-particle contact forces $\boldsymbol{f}^\alpha$ for $\alpha = 1, 2, \ldots, N_c$. Note only inter-particle forces are used in the Christoffersen et al. expression, which is a good approximation when the number of particle in the array N_p is large.

The above results present a unified case for the linkage between macroscopic stresses and inter-particle forces and highlight the importance of GEM. Even though the expression by Christoffersen et al. [23] has been around for decades, obtaining values for the inter-particle forces has been difficult in real granular materials. The only available technique until now has been photoelasticity [26,27] and has been used on disks fabricated with birefringent material [24,25]. For example, Majmudar and Behringer [25] have used this technique to back-calculate the value of the contact forces in birefringent discs loaded in the laboratory. The introduction of GEM and its potential use with 3DXRD and 3DXRCT opens the door to obtaining inter-particle contact forces in real granular materials and the use of expressions as those shown in Eq. (13) will enable the connection between inter-particle forces in natural materials and average macroscopic stresses for the first time. Average macroscopic stresses can then be used as in Andrade et al. [20] to obtain the evolution of key material parameters, such as friction and dilatancy, which serve as the prelude to the development of physics-based constitutive models for real granular materials.

Remark 7 It has been noted that the average stress in granular media may be asymmetric [34]. However, if the average stress $\langle \boldsymbol{\sigma} \rangle$ is defined as in Eq. (11), stemming from static equilibrium and without accounting for couples, the resulting stress is symmetric as a consequence of the symmetric average particle stress. This is an important consideration, since the symmetry of the continuum stress measures is central to most constitutive theories and finite element procedures.

5 Numerical examples

In this section we present two numerical examples representative of the capabilities of the granular element method (GEM). The main goal of this section is not to validate the method, but rather verify it. We shall validate the method using physical tests in granular materials in a forthcoming publication. An important objective of this section is to show examples where data similar to that extracted from actual experiments is used in conjunction with GEM. As mentioned before, GEM necessitates input about the fabric of the granular assembly and the average stresses (or average strains) in each particle in the assembly. It has been shown that the information necessitated by GEM can be extracted experimentally (see, for example, [19,22]). In this paper, we extract the aforementioned input information from numerical experiments using finite elements and discrete elements. By doing this, we not only verify the accuracy of the method, but also clearly demonstrate the process to link GEM and the necessary input data. In particular, a finite element example is used to exemplify the procedure to be used in the future, where fabric and average particle strains can be extracted from macroscopic experiments such as those cited above. The finite element example serves as a mapping for the concept shown in Fig. 1. Here, we use the particle elasticity to obtain average particle stresses from average particle strains via $\bar{\boldsymbol{\sigma}}^p = \boldsymbol{c} : \bar{\boldsymbol{\epsilon}}^p$. Once again, exploiting the concept of force and using particles as strain gauges.

We focus our attention on 2D examples for simplicity and clarity of presentation, but emphasize the full three-dimensionality of the method. The first example uses finite elements to extract average stresses and the second example uses discrete element method (DEM). Both FEM and DEM furnish direct numerical simulations (DNS) that not only produce input for GEM in the form of average stresses, but also produce contact forces and global stresses to verify the response obtained from GEM. The examples use FEM and DEM to demonstrate the ability of GEM to work with *any* method (including experiments) that can produce average particle stresses. Also, the FEM and DEM simulations use angular and perfectly circular particles to showcase the ability of the method to work with irregular shapes. Finally, infinite friction and smooth contacts are modeled in the examples to test the method under extreme frictional scenarios.

5.1 Odometric compression of angular particles

In this example, a simple odometric compression test is performed using FEM and GEM. Odometric compression is defined here as a macroscopic deformation in the vertical component with all other strain components vanishing. Hence, the only non-zero macroscopic strain component is the vertical component. The array and the specified boundary conditions are shown in Fig. 6. The sample is compressed by a specified stress of 0.5 MPa on the top face. All faces of the sample are considered rigid and smooth. Only the top face

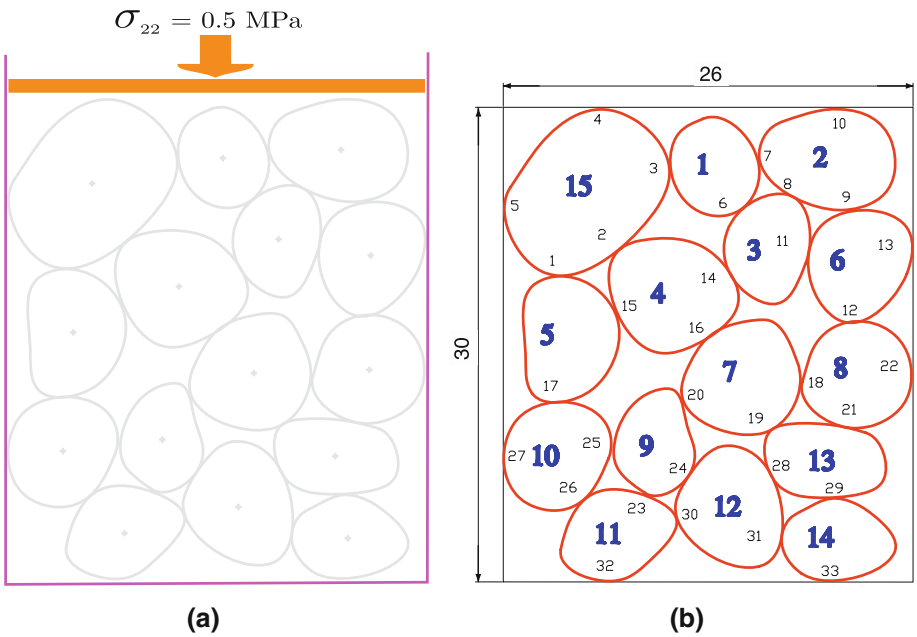

Fig. 6 Odometric test configuration. **a** Array fabric and boundary conditions. *Top* face (*orange*) is prescribed a vertical stress of 0.5 MPa using a smooth, rigid wall. *Bottom* and lateral faces (*purple*) are stationary, smooth and rigid walls, hence producing macroscopic odometric compression in the sample. **b** Sample dimensions in millimeters, particle numbers and contact point numbers

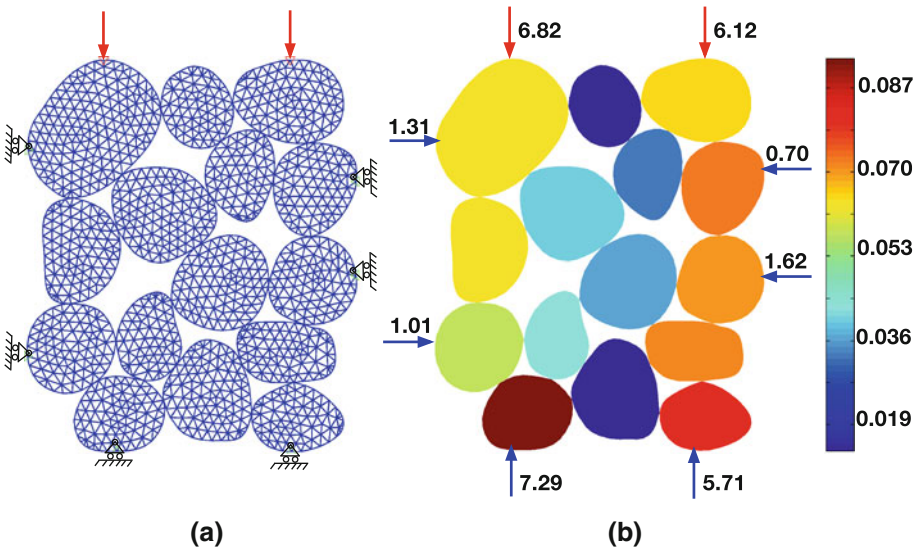

Fig. 7 **a** Finite element mesh and modeling boundary conditions for odometric test. **b** L_2-norm of the average particle strains calculated from finite elements. Forces are in Newtons

in this example is allowed to displace vertically as a result of macroscopic deformation.

The sample's geometry and fabric characteristics are also shown in Fig. 6 for illustrative purposes. For instance, it can be seen that the sample is comprised of $N_p = 15$ particles of angular shape. There are $N_c = 33$ contacts in the entire array so that $\eta = \{1, 2, 3, \ldots, 33\}$ and also $\eta_{g1} = \eta_{g2} = \{4, 10\}$ since both components of force are prescribed on these boundary nodes. Therefore, the active set η_A contains all contact points in the array, except for points 4 and 10 which belong to Γ_t where tractions are prescribed. Furthermore, the array is statically indeterminate, with $3N_p = 45$ equations stemming from static equilibrium in each particle. However, there are 31 nodes in the active set with 2 degrees of freedom each, making the total number of unknowns in the system 62. As mentioned before, in 2D, GEM furnishes $6N_p$ equations, which in this case make 90 equations of equilibrium and linear momentum from each particle. Clearly, in this case $N_c/N_p = 33/15 < 3$ as required by the method. We should note that $N_c/N_p = 2.2$ in this case, which is lower than the average coordination number in the array, 3.87.

A finite element simulation is carried out with a mesh shown in Fig. 7. Triangular elements are used to discretize the particles shown in Fig. 6 and the grains are assumed to be linear elastic with Young's modulus of 1 GPa and a Poisson's ratio of 0.3. Also, the inter-particle friction coefficient is assumed to be infinite so that particles cannot slide relative to each other. This latter assumption simplifies the finite element simulations considerably as it bypasses contact analysis. As shown in Fig. 7, there are eight nodes in contact with

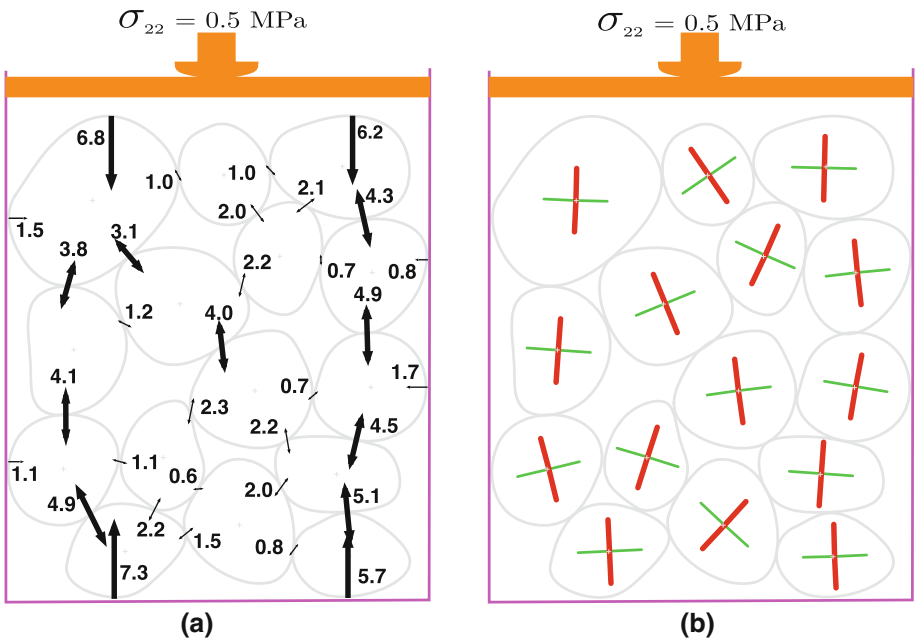

Fig. 8 Granular element method results: **a** contact forces in Newtons and **b** average principal stresses and directions in each particle (*red, thicker lines* are major principal stresses; *green, thinner lines* are minor principal stresses)

the boundary of the sample. Vertical forces are prescribed in the top two nodes to capture the prescribed pressure of 0.5 MPa, whereas reaction forces are calculated for the other six nodes in contact with the smooth stationary walls. The corresponding prescribed and reaction forces at the boundary forces are shown in Fig. 7. Also, the average granular strains, corresponding to the current macroscopic loading, are computed and their magnitude (L_2-norm) is plotted in Fig. 7. These average (tensorial) strains and the given granular fabric (particle shapes and contact point location) are taken as input parameters for GEM analysis. The strains are readily converted to stresses via the generalized Hooke's law, i.e., $\bar{\boldsymbol{\sigma}}^p = \boldsymbol{c} : \bar{\boldsymbol{\epsilon}}^p$. This process is similar to the one to be followed when GEM is used in conjunction with experiments where fabric and average particle strains are obtained under macroscopic loading (e.g., 3DXRCT and 3DXRD).

Figure 8 shows the results obtained using GEM. Contact forces are plotted in the figure and can be compared with those obtained at the boundary from FEM analysis. Clearly, GEM is capturing the contact forces (at least on the boundaries) accurately. From these contact forces, the principal stress components and directions can be obtained at the particle level. The principal directions of the average particle stresses are shown in Fig. 8 and help depict the appearance of the so-called load-chains [25]. Quantitatively, one can define force chains as the average direction of principal stresses, which have to be parallel to the principal stress directions [35]. In the particular case shown here, the most compressive direction is the vertical direction and this is clearly shown by the force chains depicted in Fig. 8. Finally, we can compute the average stress $\langle \boldsymbol{\sigma} \rangle$ as defined in Eq. (11). The apparent macroscopic stress obtained from the FEM simulation shown in Fig. 7 yields a biaxial compressive state of stress with 0.5 MPa in the vertical (prescribed) direction and 0.08 MPa in the horizontal direction. On the other hand,

$$\langle \boldsymbol{\sigma} \rangle = \begin{bmatrix} -0.085 & 0.001 \\ 0.001 & -0.496 \end{bmatrix} \text{MPa}$$

as obtained from Eq. (11), which is very close to the macroscopic stress from FEM and represents a quasi-odometric state of stress in the granular assembly.

5.2 Biaxial compression of circular particles

This example features a mono-disperse array of discs 1 mm in diameter. The assembly and the boundary conditions imposed are shown in Fig. 9. The simple packing is biaxially loaded and the direct numerical simulation is performed using discrete element method (DEM). The method was endowed with normal and tangential stiffness $k_n = 100$ kN/mm and $k_t = k_n$, respectively. Also, there is no frictional resistance between the particles, so particle slippage is imminent. DEM is used to compute inter-particle forces under quasi-static conditions. These inter-particle forces obtained from DEM are shown in Fig. 9, which also plots the average particle stresses produced from DEM. These inter-particle forces furnish the acid test for GEM as the method should accurately represent these forces if it is to prove accurate. Also, the average stresses extracted from DEM are a necessary input for GEM.

Using the fabric for the array shown in Fig. 9, GEM is implemented while representing the same boundary conditions imposed during the DNS phase, i.e., biaxial macroscopic stresses of 4.15 MPa in the vertical direction and

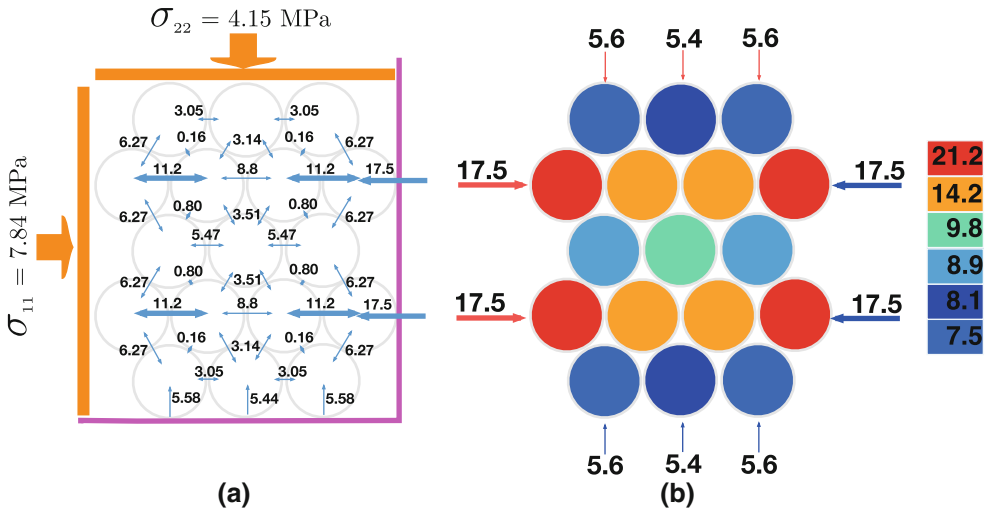

Fig. 9 Biaxial test configuration. **a** Particle array fabric and boundary conditions with contact forces from DEM. *Top* and *left* (*orange*) faces are prescribed tractions via rigid, smooth walls. *Bottom* and *right* (*purple*) faces are rigid, smooth and stationary. **b** L_2-norm of the average particle stresses calculated using DEM

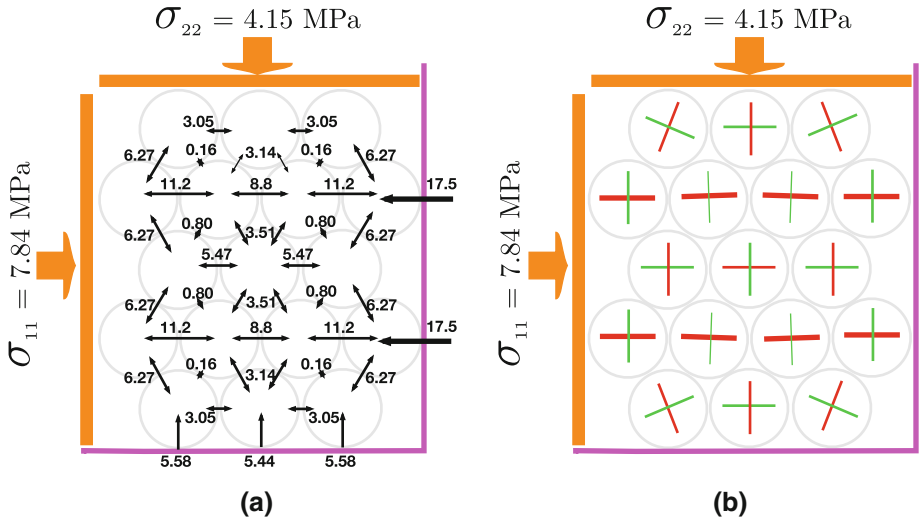

Fig. 10 Granular element method results: **a** contact forces and **b** average principal stresses and directions in each particle (*red, thicker lines* are major principal stresses; *green, thinner lines* are minor principal stresses). Comparing with contact forces from DEM, the results are identical

7.84 MPa in the horizontal direction. These stress boundary conditions are implemented via contact forces with the particles on the pressure faces of the sample as shown in Fig. 10. The average stresses from DEM are also used as input for the calculations. As before, GEM is used to obtain the contact forces in the idealized array. The resulting contact forces are depicted in Fig. 10. Comparing these with those obtained from DEM and depicted in Fig. 9, it can be observed that the inter-particle forces obtained by DEM and GEM are practically identical. Also shown in Fig. 10 is the principal directions and magnitudes of the average stresses on each particle. It can be clearly noted that two load chains emerge in the horizontal direction (macroscopic mean compressive direction). These load chains act as 'pillars' for the array, with the other particles providing stability support. Finally, the average macroscopic stress in the array is calculated using Eq. (11) yielding

$$\langle \boldsymbol{\sigma} \rangle = \begin{bmatrix} -7.84 & 0 \\ 0 & -4.15 \end{bmatrix} \text{MPa}$$

which exactly coincides with the imposed boundary stress.

The presented results showcase the ability of the method to obtain inter-particle forces accurately in irregular granular arrays under macroscopic loading. We have used FEM and DEM as examples of methods that can provide the necessary information for GEM: fabric and average stresses. With this information in hand, GEM can obtain inter-particle forces that can then be used to calculate average stresses within macroscopic volumes.

6 Conclusion

We have presented a new method called the granular element method (GEM) which enforces static equilibrium and balance of linear momentum in each particle within a macroscopic array. These set of equations render most particle arrays tractable, in general, as there are usually more equations than unknown contact forces. Therefore, if a solution exists, it will be unique. The method takes as necessary input the fabric of the granular assembly (shape of particles and contact points) and the average stresses in each particle of the array. This information can be obtained from advanced experiments using X-ray CT and X-ray diffraction already available for natural granular materials such as sands. It is anticipated that GEM will be used in future experiments to be able to infer the inter-particle contact forces in real assemblies under macroscopic loads. These inter-particle forces can the be used to obtain average macroscopic measures of stress in the array, providing a missing link in granular matter in order to connect continuum representations and the discrete states. This will in turn spur further development of multiscale methods and physics-based constitutive models for granular materials.

Acknowledgements Support for this work was partially provided by NSF Grant No. 1060087, AFOSR Grant No. FA9550-11-1-0052, and DOE Grant No. DE-FG02-08ER15980. This support is gratefully acknowledged.

References

1. Andrade, J.E., Borja, R.I.: Capturing strain localization in dense sands with random density. Int. J. Numer. Methods Eng. **67**, 1531–1564 (2006)
2. Andrade, J.E., Ellison, K.C.: Evaluation of a predictive constitutive model for sands. J. Geotech. Geoenviron. Eng. **134**, 1825–1828 (2008)
3. Dafalias, Y.F., Popov, E.P.: A model of nonlinearly hardening materials for complex loadings. Acta Mech. **21**, 173–192 (1975)
4. Grueschow, E., Rudnicki, J.W.: Elliptic yield cap constitutive modeling for high porosity sandstone. Int. J. Solids Struct. **42**(16–17), 4574–4587 (2005)
5. Manzari, M.T., Dafalias, Y.F.: A critical state two-surface plasticity model for sands. Géotechnique **43**, 255–272 (1997)
6. DiMaggio, F.L., Sandler, I.S.: Material model for granular soils. J. Eng. Mech. Div. ASCE **97**, 935–950 (1971)
7. Bažant, Z.P., Caner, F.C., Carol, I., Adley, M.D., Akers, S.A.: Microplane model M4 for concrete. I: formulation with work-conjugate deviatoric stress. J. Eng. Mech. **126**, 944–953 (2000)
8. Schofield, A., Wroth, P.: Critical State Soil Mechanics. McGraw-Hill, New York (1968)
9. Cundall, P.A., Strack, O.D.L.: A discrete numerical model for granular assemblies. Géotechnique **29**, 47–65 (1979)
10. Bardet, J.P., Proubet, J.: Adaptive dynamic relaxation for statics of granular materials. Comput. Struct. **39**, 221–229 (1991)
11. Rothenburg, L., Bathurst, R.J.: Analytical study of induced anisotropy in idealized granular materials. Géotechnique **39**, 601–614 (1989)
12. Jensen, R.P., Bosscher, P.J., Plesha, M.E., Edil, T.B.: DEM simulation of granular media—structure interface: effect of surface roughness and particle shape. Int. J. Numer. Anal. Methods Geomech. **23**, 531–547 (1999)
13. Tu, X., Andrade, J.E.: Criteria for static equilibrium in particulate mechanics computations. Int. J. Numer. Methods Eng. **75**, 1581–1606 (2008)
14. Oda, M., Takemura, T., Takahashi, M.: Microstructure in shear band observed by microfocus X-ray computed tomography. Géotechnique **54**, 539–542 (2004)
15. Alshibli, K.A., Sture, S., Costes, N.C., Frank, M.L., Lankton, F.R., Batiste, S.N., Swanson, R.A.: Assessment of localized deformations in sand using X-ray computed tomography. Geotech. Test. J. ASCE **23**, 274–299 (2000)
16. Ketcham, R.A., Carlson, W.D.: Acquisition, optimization and interpretation of X-ray computed tomographic imagery: applications to the geosciences. Comput. Geosci. **27**, 381–400 (2001)
17. Wang, L., Park, J.Y., Fu, Y.: Representation of real particles for DEM simulation using X-ray tomography. Constr. Build. Mater. **21**, 338–346 (2005)
18. Poulsen, H.F.: Three-Dimensional X-Ray Diffraction Microscopy: Mapping Polycristals and their Dynamics. Springer, New York (2004)
19. Hall, S.A., Bornert, M., Desrues, J., Pannier, Y., Lenoir, N., Viggiani, G., Bésuelle, P.: Discrete and continuum analysis of localized deformation in sand using X-ray micro CT and volumetric digital image correlation. Géotechnique **60**, 315–322 (2010)
20. Andrade, J.E., Avila, C.F., Lenoir, N., Hall, S.A., Viggiani, G.: Multiscale modeling and characterization of granular matter: from grain scale kinematics to continuum mechanics. J. Mech. Phys. Solids **59**, 237–250 (2011)
21. Martins, R.V., Margulies, L., Schmidt, S., Poulsen, H.F., Leffers, T.: Simultaneous measurement of the strain tensor of 10 individual grains embedded in an Al tensile sample. Mater. Sci. Eng. A **387**(389), 84–88 (2004)
22. Hall, S.A., Wright, J., Pirling, T., Andò, E., Hughes, D.J., Viggiani, G.: Can intergranular force transmission be identified in sand? Granul. Matter (2011). doi:10.1007/s10035-011-0251-x
23. Christoffersen, J., Mehrabadi, M.M., Nemat-Nasser, S.: A micromechanical description of granular material behavior. J. Appl. Mech. **48**, 339–344 (1981)
24. Drescher, A., de Josselin de Jong, G.: Photoelastic verification of a mechanical model for the flow of a granular material. J. Mech. Phys. Solids **20**, 337–340 (1972)
25. Majmudar, T.S., Behringer, R.P.: Contact force measurements and stress-induced anisotropy in granular materials. Nature **435**, 1079–1082 (2005)
26. Frocht, M.M.: Photoelasticity, vol. 1. Wiley, New York (1941)
27. Frocht, M.M.: Photoelasticity, vol. 2. Wiley, New York (1941)
28. Pellegrino, S.: Structural computations with the singular value decomposition of the equilibrium matrix. Int. J. Solids Struct. **30**, 3025–3035 (1993)
29. Holzapfel, G.A.: Nonlinear Solid Mechanics. Wiley, West Sussex (2000)
30. Peña, A.A., Lind, P.G., Herrmann, H.J.: Modeling slow deformation of polygonal particles using dem. Particuology **6**, 506–514 (2008)
31. Hughes, T.J.R.: The Finite Element Method. Prentice-Hall, Englewood Cliffs (1987)
32. Strang, G.: Linear Algebra and Its Applications. 3rd edn. Thomson Learning, London (1988)
33. Belytschko, T., Liu, W.K., Moran, B.: Nonlinear Finite Elements for Continua and Structures. Wiley, West Sussex (2000)
34. Bardet, J.P., Vardoulakis, I.: The asymmetry of stress in granular media. Int. J. Solids Struct. **38**, 353–367 (2001)
35. Peters, J.F., Muthuswasmy, M., Wibowo, J., Tordesillas, A.: Characterization of force chains in granular material. Phys. Rev. E **72**, 041397 (2005)